bioRxiv preprint doi: https://doi.org/10.1101/2020.09.22.307421; this version posted September 22, 2020. The copyright holder for this preprint (which was not certified by peer review) is the author/funder. All rights reserved. No reuse allowed without permission.

Mouse Single Pancreatic β Cell Transcriptomics Reveal Sexual Dimorphism of Transcriptomes and Identify Sex-dependent Type 2 Diabetes Altered Genes

Gang Liu[1,2,#,a], Yana Li[3,4,#,b], Tengjiao Zhang[1,#,c], Mushan Li[5,#,d], Sheng Li[1,2,e], Shuxin Liu[1,2,f], Minglu Xu[1,2,g], Zhen Shao[3,*,h], Weiyang Shi[6,*,i], Weida Li[1,2,*,j]

[1]*Frontier Science Center for Stem Cell Research, School of Life Sciences and Technology, Tongji University, Shanghai 200092, China.*

[2]*Tsingtao Advanced Research Institute, Tongji University.*

[3]*CAS Key Laboratory of Computational Biology, CAS-MPG Partner Institute for Computational Biology, Shanghai Institute of Nutrition and Health, Chinese Academy of Sciences, Shanghai 200031, China.*

[4]*University of Chinese Academy of Sciences, Beijing 100049, China.*

[5]*Department of Statistics, The Pennsylvania State University, University Park, Pennsylvania 16802, USA.*

[6]*Ministry of Education Key Laboratory of Marine Genetics and Breeding, College of Marine Life Sciences, Ocean University of China, Tsingtao Shandong 266003, China.*

 # Equal contribution

**Correspo*ndence

E-mail: shaozhen@picb.ac.cn (Shao Z), wshi@ouc.edu.cn (Shi W), liweida@tongji.edu.cn (Li W).

Running title: *Gang L et al /Mouse Single Pancreatic β Cell Transcriptomics Reveal Sexual Dimorphism of Transcriptomes and Identify Sex-dependent Type 2 Diabetes Altered Genes*

bioRxiv preprint doi: https://doi.org/10.1101/2020.09.22.307421; this version posted September 22, 2020. The copyright holder for this preprint (which was not certified by peer review) is the author/funder. All rights reserved. No reuse allowed without permission.

[a]ORCID: 0000-0003-1401-9215.

[b]ORCID: 0000-0002-3386-9090.

[c]ORCID: 0000-0001-7815-2504.

[d]ORCID: 0000-0003-2727-950X.

[e]ORCID: 0000-0002-6126-8866.

[f]ORCID: 0000-0002-4664-5512.

[g]ORCID: 0000-0001-6817-3109.

[h]ORCID: 0000-0002-4934-4360.

[i]ORCID: 0000-0002-1805-6884.

[j]ORCID: 0000-0001-6578-6321.

Total word counts (from Introduction to Conclusions): 3363

Total figures: 7

Total tables: 4

Total supplementary figures: 3

Total supplementary tables: 3

Total supplementary files: 6

bioRxiv preprint doi: https://doi.org/10.1101/2020.09.22.307421; this version posted September 22, 2020. The copyright holder for this preprint (which was not certified by peer review) is the author/funder. All rights reserved. No reuse allowed without permission.

Abstract

Type 2 diabetes, characterized by malfunction of pancreatic β cells, is affected by multiple cues including sex differences. Nevertheless, mechanisms of sex differences in type 2 diabetes susceptibility and pathogenesis remain unclear. Using single-cell RNA sequencing (scRNA-seq) technology, we showed that sexual dimorphism of transcriptome exists in mouse β cells. Our analysis further revealed the existence of sex-dependent type 2 diabetes altered genes in high fat diet induced T2D model, suggesting divergences in pathological mechanisms of type 2 diabetes between sexes. Our results indicated that sex should be taken into consideration when treating diabetes, which was further validated by the sex-matched and sex-mismatched islet transplantation in mice. Compared to sex-matched transplants, sex-mismatched transplants showed downregulation of genes involved in the longevity regulating pathway in β cells and led to impaired glucose tolerance in diabetic mice. Taken together, our findings could advance current understanding of type 2 diabetes pathogenesis with sexually dimorphic perspectives and provide new insights to the development of precision medicine.

KEYWORDS: Type 2 diabetes mellitus; Pancreatic β cell; Sex-biased gene expression; Sex-dependent T2D altered genes; Precision medicine

Introduction

The efficacy of current anti-diabetic medication varies significantly among individuals with diabetes, highlighting the importance of personalized treatment for type 2 diabetes (T2D). However, the bottleneck for precision medicine lies in the heterogeneous nature of the disease, which not only hinges on genetic predispositions that have been

bioRxiv preprint doi: https://doi.org/10.1101/2020.09.22.307421; this version posted September 22, 2020. The copyright holder for this preprint (which was not certified by peer review) is the author/funder. All rights reserved. No reuse allowed without permission.

identified by GWAS (Genome Wide Association Study), but also other cues, including sex, diet, and aging. Among these factors, sex differences should be first considered for personalized therapy since sex is one of the most recognizable traits.

However, in most current studies on metabolism using rodents, female animals are usually neglected, because male animals have the tendency to show better disease phenotypes and are dominantly used [1]. And this experimental bias on sex hampered novel and comprehensive acknowledgement of metabolic pathological mechanisms. Thus, the National Institutes of Health (NIH) demands sex differences should be emphasized in preclinical studies [2, 3], which should be especially stressed in T2D as a global pandemic.

Glucose homeostasis is controlled by pancreatic islet, which is mainly composed of α cells, β cells, δ cells and PP cells. α cells elevate glucose level by secreting glucagon to promote hepatic glucose synthesis, and β cells release insulin to decrease glucose level by stimulating blood glucose uptake by fat, muscle, liver, and intestine cells, etc. δ cells secret somatostatin to downregulate hormones releasing from both α cells and β cells via paracrine signaling [4]. Polypeptide from PP cells, the most infrequent islet cell type, has effects on both gastric and pancreatic secretions [5].

Despite the similar cell type components of islet architecture shared by both male and female, there exist profound sex differences in islet physiological function and metabolism, signaling pathways involved in hormone releasing, and diabetes occurrence [6]. For example, female rats are more susceptible than males to streptozotocin (STZ) induced diabetes, suggesting that female rat β cells are more sensitive to STZ toxicity than male β cells [6]. Similarly, maternal high fat diet results in insulin resistance and oxidative stress-induced β cell loss specifically in male offsprings, rather than in female offsprings, indicating that female islets might have self-protective machinery against oxidative stress [7]. In human, type 2 diabetes occurs more frequently in men with younger age and less BMI than women [8-10]. Insulin sexual dimorphism of DNA methylation was also observed in human islets by whole

bioRxiv preprint doi: https://doi.org/10.1101/2020.09.22.307421; this version posted September 22, 2020. The copyright holder for this preprint (which was not certified by peer review) is the author/funder. All rights reserved. No reuse allowed without permission.

112 islet genome-wide DNA methylation sequencing. It is suggested that sex differences of
113 methylome are associated with differences of islet genes expression and insulin
114 secretion level [11]. However, sexual dimorphism of pancreatic islet β cell has not been
115 investigated at the single cell level, and these studies could reveal sex differences of
116 gene expression in islet β cells between male and female and provide better treatment
117 plans for diabetic patients from both sex groups.

118 Sex differences in diabetes susceptibility, development and progression have been
119 previously reported, suggesting the existence of sex-dependent diabetes associated
120 genes. Previous studies showed that androgen receptor specifically expressed in male
121 islet β cells and plays an important role in regulating glucose-stimulated insulin
122 secretion in both mice and humans [12]. It has also been reported that *KLF14* allele
123 variants show increased female-specific T2D risk, probably via female-specific fat
124 storage and distribution [13]. Recent banding studies reported that single-cell RNA
125 sequencing technology has been applied to identify novel diabetes altered genes [14-
126 16]. Nevertheless, the diverse sex-dependent diabetes associated genes and molecular
127 pathways have not been comprehensively investigated from these studies.

128 Here, we systematically analyzed the single cell gene expression profiles of healthy
129 and diabetic β cells from mice. We found a considerable number of genes had sex-
130 biased expression in β cells. Furthermore, we identified 122 sex-dependent diabetes
131 altered genes, suggesting that the molecular mechanisms mediating diabetes
132 pathogenesis in males and females have important differences. Based on the recognition
133 of the sex differences in T2D altered genes and pathways in β cells, we concluded that
134 sex as a biological variance should be emphasized in diabetes treatment. And this
135 conclusion was further supported by the sex-matched and sex-mismatched islet
136 transplantation in mice. Compared to sex-matched transplants, we found that genes
137 involved in the longevity regulating pathway tended to be down-regulated in β cells of
138 sex-mismatched transplants, and glucose tolerance notably decreased in diabetic mice
139 transplanted with sex-mismatched islets. Together, our results not only advanced

bioRxiv preprint doi: https://doi.org/10.1101/2020.09.22.307421; this version posted September 22, 2020. The copyright holder for this preprint (which was not certified by peer review) is the author/funder. All rights reserved. No reuse allowed without permission.

current understanding of T2D pathogenesis, but also provided new insights and targets for developing sex-dependent precision medicine to treat diabetes.

Results

Identification of male and female pancreatic β cell transcriptomes in mouse

To obtain expression profiles of mouse pancreatic β cells, we employed flow cytometry to isolate single islet cells from dissociated mouse islets with live dye staining (**Figure 1A**). Totally, we collected and sequenced 5472 islet cells (3264 male; 2208 female) from both male and female mice, including 1056 islet cells (1056 male; 768 female) of 8-week-old healthy mice, 2208 islet cells (1152 male; 1056 female) of 9-month-old healthy and diabetic mice, 672 male transplanted islet cells (9 months post-transplant) in kidney capsules of both male and female recipient mice, and 768 endogenous pancreatic islet cells (384 male; 384 female) of recipient mice (detailed sample information in **Table 1**). Single-cell RNA sequencing library was constructed by a modified Smart-seq2 protocol. The average library size is 370K reads per cell, and the average number of genes detected in these cells is about 1500 per cell. We retained 4662 cells that have at least 500 genes detected (Figure S1A). The retained cells had high total counts of unique molecular identifiers (UMIs) mapped to gene exons (Figure S1B), and low fractions of UMI counts of mitochondrial genes (Figure S1C), suggesting we obtained a set of qualified scRNA-seq profiles of mouse islet for the main purpose of this study.

From these 4662 cells, we went on to identify β cells for downstream analysis. Firstly, we applied an adjusted CPM method (adjCPM) to normalize our scRNA-seq data by excluding the union of the top 2 genes with the highest expression from all cells while calculating the normalization factors (Figure S1D and S1E; see Methods). Secondly, hierarchal clustering of scRNA-seq profiles based on the union of the top 10 highly expressed genes from all cells was used to discriminate the identity of the cells (Figure S1F). After performing principal component analysis with the identified hyper

bioRxiv preprint doi: https://doi.org/10.1101/2020.09.22.307421; this version posted September 22, 2020. The copyright holder for this preprint (which was not certified by peer review) is the author/funder. All rights reserved. No reuse allowed without permission.

variable genes (HVGs) and subsequent visualization by t-distributed stochastic neighbor embedding (t-SNE) (Figure S1G; see Methods), the retained islet cells of healthy (8-week-old; 9-month-old) and diabetic mice were found to be aggregated into two clusters exhibiting differential expression of β cell marker gene *Ins2* (**Figure 1B and 1C**). Then, 3912 β cells (2197 male; 1715 female) from mice in different conditions were identified through high expression of *Ins2* (Figure 1C and S4A). The sex of mouse β cells was labeled on the t-SNE map (male in blue; female in red; **Figure 1D**), and further confirmed by X and Y chromosome genes (Figure S2B). We found male and female β cells were not completely overlapped on the t-SNE plot (Figure 1D). To verify the existence of sexually dimorphic gene expression, we applied Kolmogorov-Smirnov test (K-S test) to analyze the differential expression of *Ins2* between male and female β cells, and found its expression was significantly different between two sexes (Figure 1D), indicating sexual dimorphism of β cell transcriptomes exist in mouse and could be important to β cell functions.

Sex-biased gene expressions in mouse β cells under healthy and T2D conditions

To identify genes that display sex-biased expression pattern in mouse pancreatic β cells, we first compared the transcriptional profiles of male β cells with female β cells from 8-week-old C57BL/6J mice (**Figure 2A**). Differentially expressed genes were sorted out by MAST [17], with a FDR cutoff of 0.05 (the same cutoffs were used for all the differential analysis using MAST in our study). In total, we obtained 162 differentially expressed genes (DEGs), comprising 37 genes expressed higher in male and 125 genes expressed higher in female (Figure 2A). Among them, only four genes were on the sex chromosomes, including X chromosome (*Xist*) and Y chromosome (*Eif2s3y*, *Ddx3y*, *Uty*) (**Figure 2B**), suggesting that considerable level of sexual dimorphism exist in healthy β cell transcriptomes.

To investigate whether such sexually dimorphic β cell transcriptomes also exist in diabetic conditions, β cells from high-fat-diet (HFD) induced diabetic mice were

bioRxiv preprint doi: https://doi.org/10.1101/2020.09.22.307421; this version posted September 22, 2020. The copyright holder for this preprint (which was not certified by peer review) is the author/funder. All rights reserved. No reuse allowed without permission.

collected for scRNA-seq. Firstly, we used HFD to induce T2D model with β cell failure in C57BL/6J mice (fed with HFD from 8-week-old) as previously described [18]. Consequently, characteristic T2D phenotypes were observed in those diabetic mice of both male and female, including high body weight, increased fasting insulin level, and impaired glucose tolerance. Notably, sex differences of T2D were also observed: the fasting serum insulin level of healthy male mice is significantly higher than healthy female mice (**Figure 2C**). In addition, the area under curve (AUC) of glucose tolerance test showed that the impairment of glucose tolerance in female T2D mice was more significant than that in male T2D mice, as p value of female T2D <0.001 and male T2D<0.01 (**Figure 2D**). Then, to explore the genetic basis for such differences, we obtained single β cell transcriptomes from 9-month-old diabetic mice (HFD feeding up to 7 months) and age-matched healthy mice (normal diet, ND) of both sexes. The comparison of single β cell transcriptional profiles of male and female from either healthy or T2D mice was carried out by MAST with the same cutoffs as described above. As shown in the results, 394 DEGs between male and female in 9-month-old healthy mice were identified, including 200 genes expressed higher in male and 194 genes expressed higher in female. In parallel, 81 male highly expressed genes, and 52 female highly expressed genes were identified in β cells from T2D mice (**Figure 2E**).

To further elucidate sex-biased pathways based on these comparisons, gene set enrichment analysis (GSEA) was performed with the cutoff set as FDR<=0.25 (the same cutoff was used for all GSEA in our study) [19]. In β cells from both 8-week-old and 9-month-old healthy animals, the longevity regulating pathway was enriched in males, and related genes (*Ins1*, *Ins2*, *Irs2*, *Hspa1a*, *Hspa8*) were expressed significantly higher in males (**Figure 2F**; S2C and S2D). Intriguingly, the ribosome pathway was consistently enriched in females in β cells from both healthy (8-week-old; 9-month-old) and diabetic mice (Figure S2C; S2D and S2E). Importantly, in β cells from diabetic mice, both the N-Glycan biosynthesis pathway and Notch signaling pathway were enriched in males. Conversely, the JAK-STAT signaling pathway, ferroptosis pathway,

bioRxiv preprint doi: https://doi.org/10.1101/2020.09.22.307421; this version posted September 22, 2020. The copyright holder for this preprint (which was not certified by peer review) is the author/funder. All rights reserved. No reuse allowed without permission.

spliceosome pathway, carbohydrate digestion and absorption pathway were enriched in female β cells from diabetic mice (Figure S2E). Expression patterns of representative sex-biased DEGs involved in the GSEA results were shown in the heatmap (Figure 2F). Above all, our results validated the existence of sex-biased gene expression in β cells of both healthy and diabetic mice, indicating that the pathological mechanism of T2D might differ between males and females.

Abundant sex-dependent T2D altered genes were found in mouse β cells

Given the sex-biased gene expressions detected in T2D β cells, we hypothesized T2D development may differ in males and females. Previous studies compared the single-cell transcriptional profiles of T2D islets with that of healthy islets to identify T2D altered genes [14-16] without considering the factor of sex. To dissect that in a sex-dependent manner, we compared the single-cell transcriptome of β cells from T2D mice with that from age-matched healthy mice. Firstly, we did a sex-independent comparison, in which β cells from both sexes were used for differential analysis, and we defined 98 sex-independent genes. Then, we compared the diabetic β cells with healthy β cells of the same sex to obtain DEGs in either male or female specific manner, and consequently compared the DEGs of each sex with the 98 sex-independent genes. The non-overlapping parts were defined as sex-dependent T2D altered genes, including 57 female-dependent and 66 male-dependent genes (**Figure 3A** and **3B**), among which the *Spc5* was upregulated in female diabetic β cells but down-regulated in male diabetic β cells (Figure S3A).

To note, among the female-dependent T2D altered genes, the top 5 up-regulated genes were *Fxyd2*, *Hsp8*, *Cpe*, *G6pc2* and *Serp1*, while the top 5 down-regulated genes were *Sdf2l1*, *Ssr4*, *Shisal2b*, *Chac1*, *Ewsr1* (Figure S3A). Notably, according to previous reports, the *Fxyd2* knock-out mice showed significantly improved glucose tolerance and enlarged islet size, suggesting its negative regulation of islet growth [20]. *Hsp8*/*HSC70* encodes the heat-shock cognate protein 70, which was recognized as an

bioRxiv preprint doi: https://doi.org/10.1101/2020.09.22.307421; this version posted September 22, 2020. The copyright holder for this preprint (which was not certified by peer review) is the author/funder. All rights reserved. No reuse allowed without permission.

endogenous danger signal in β cell to trigger inflammation in diabetes [21]. *Cpe* encodes Carboxypeptidase E, which plays a role in insulin synthesis by regulating proinsulin to insulin conversion for insulin synthesis [22]. The upregulation of *Cpe* was in line with the increased fasting serum insulin level observed in the T2D mice (Figure 2C). The *G6pc2* has been reported to be a negative regulator for glucose stimulated insulin secretion in mice, and its deletion results in female specific body fat reduction [23], which supports our concept of sex-dependent T2D altered gene.

In parallel, among the male-dependent T2D altered genes, the top 5 genes up-regulated in T2D were *Iapp*, *P4hb*, Rps29, *Trpm5*, and *Gabbr2*, while the top 5 genes down-regulated in T2D were *Cox4i1*, *Malat1*, *Ubb*, *Nisch*, *Ndufb7* (Figure S3A). *Iapp* encodes islet amyloid polypeptide, whose aggregation results in β cell failure and T2D onset [24]. *P4hb* encodes protein disulfide isomerase A1, whose expression is essential for maturation of proinsulin and survival of β cell in high-fat diet fed mice [25]. *Trpm5* encodes transient receptor potential channel type M5, whose deletion can reduce body weight gain and improve glucose tolerance in mice fed with high calorie diet [26].Collectively, these results demonstrated that abundant genes expression was altered under T2D diabetic condition in a sex-dependent manner.

To further systematically investigate the sex differences in T2D altered pathways, GSEA was performed based on comparison of β cells from T2D and healthy mice of each sex. In females, several pathways enriched in T2D-β cells such as pancreatic secretion pathway and longevity regulating pathway (multiple species) have direct links to β cell function and onset of T2D. Conversely, oxidative phosphorylation pathway and ribosome pathway were enriched in healthy β cells. At the same time, in males, T2D-β cells had ribosome pathway enriched and healthy β cells had type 2 diabetes mellitus pathway enriched (**Figure 3C** and **3D**). The expression patterns of genes involved in the pathways mentioned above were shown in the heatmap (**Figure 3E**) and violin plots (Figure S3B). Altogether, both the distinctive patterns of sex-dependent

bioRxiv preprint doi: https://doi.org/10.1101/2020.09.22.307421; this version posted September 22, 2020. The copyright holder for this preprint (which was not certified by peer review) is the author/funder. All rights reserved. No reuse allowed without permission.

T2D altered genes and different T2D associated pathways suggested divergence of T2D pathogenesis between sexes.

Mice with sex-matched β cell transplant exhibited better control of glucose homeostasis

Altogether, the existence of sexual dimorphism in mouse β cell transcriptome informed us that sex as an important factor in β cell function and pathogenesis of T2D should be emphasized when treating diabetes. In order to validate this critical concept, islet transplantations (an experimental treatment for insulin insufficient diabetes mellitus) with sex-matched and sex-mismatched islets were performed in mice. Male islets were isolated from 6-8 weeks old mice and transplanted into kidney capsules of age-matched male and female mice, respectively. Transplanted islets (TX-islet) and endogenous islets (Endo-islet) from recipient mice were all collected and dissociated for scRNA-seq profiling, 9 months post-transplant (**Figure 4A**). Firstly, the β cells were identified by high expression of *Ins2* as previously described (**Figure 4B**), and the transcriptomes of sex-matched and sex-mismatched transplant-β cells were compared with that of male and female endogenous β cells, respectively (**Figure 4C**). The correlation analysis revealed that the overall sex-matched transplant-β cell transcriptomes were closer to endogenous islet β cells from both male and female recipients (Figure 4C). Secondly, transplant-β cell transcriptomes were directly compared between sex-matched and sex-mismatched groups for DEGs. Sex-matched transplant-β cells had 3 genes (*Kap*, *Sfrp5* and *Akr1c21*) significantly up-regulated and 2 genes (*Ovol2*, *Matn2*) significantly down-regulated (Figure S3C and S3D). Notably, *Sfrp5* was a conservative male-biased expression gene in 8-week-old and 9-month-old healthy β cell (Table S1), previous study reported that overexpression of *Sfrp5* (down-regulated in obesity and T2D) can ameliorate impaired glucose tolerance in mice [27]. In humans, high level of serum SFRP5 was correlated with lower risk of T2D onset [28]. Moreover, the results of GSEA showed that longevity regulating pathway-multiple species was significantly

bioRxiv preprint doi: https://doi.org/10.1101/2020.09.22.307421; this version posted September 22, 2020. The copyright holder for this preprint (which was not certified by peer review) is the author/funder. All rights reserved. No reuse allowed without permission.

enriched in β cells of sex-matched transplant-islets and among the 16 leading-edge genes, *Ins2, Sod1, Sod2* and *Foxa2* are directly linked to β cell secretion (**Figure 4D**). Collectively, these results suggested that sex-matched islet transplantation could be more beneficial to the function of β cells of the transplants, thus better controlling glucose homeostasis.

To further validate the advantage of sex-matched transplantation, we transplanted islets from male and female mice into streptozotocin induced female diabetic mice, respectively (**Figure 4E**). Although the hyperglycemia (>350 mg/dl) of the diabetic recipient with sex-matched or sex-mismatched transplantation restored to normal levels 1 month post-transplant (<144 mg/dl; Figure S3E), the glucose tolerance of the diabetic mice with sex-matched transplantation was significantly better as evidenced by the oral glucose tolerance test (**Figure 4F**). Above all, our scRNA-seq analysis of β cells and experimental validation concluded that sex should be taken into consideration in diabetes treatment.

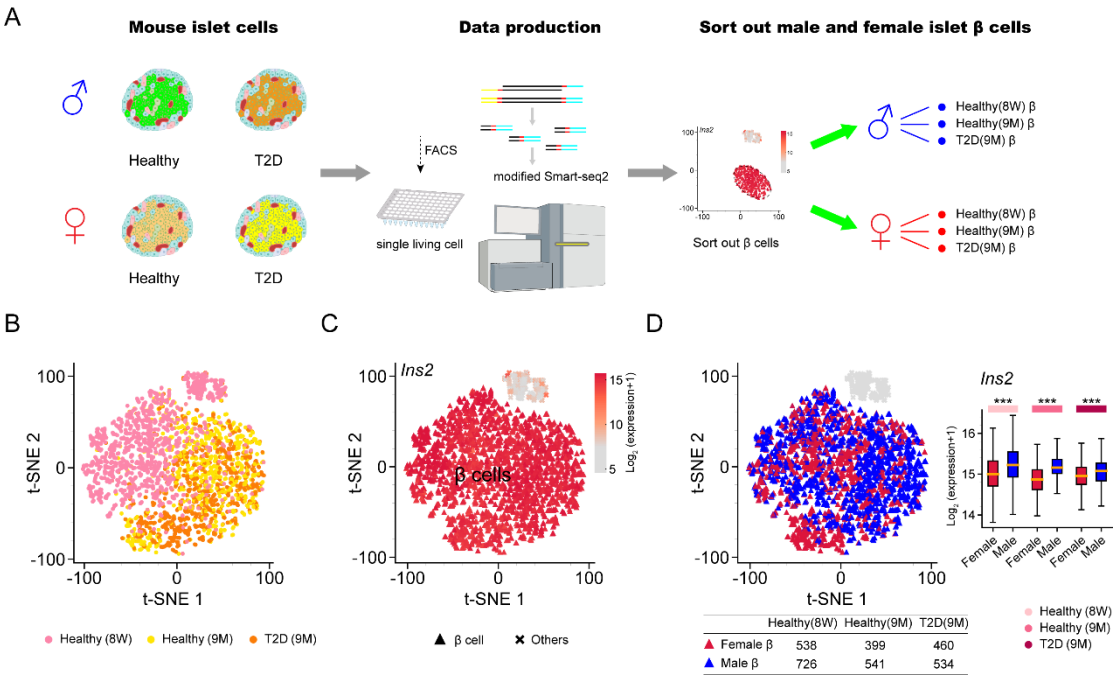

bioRxiv preprint doi: https://doi.org/10.1101/2020.09.22.307421; this version posted September 22, 2020. The copyright holder for this preprint (which was not certified by peer review) is the author/funder. All rights reserved. No reuse allowed without permission.

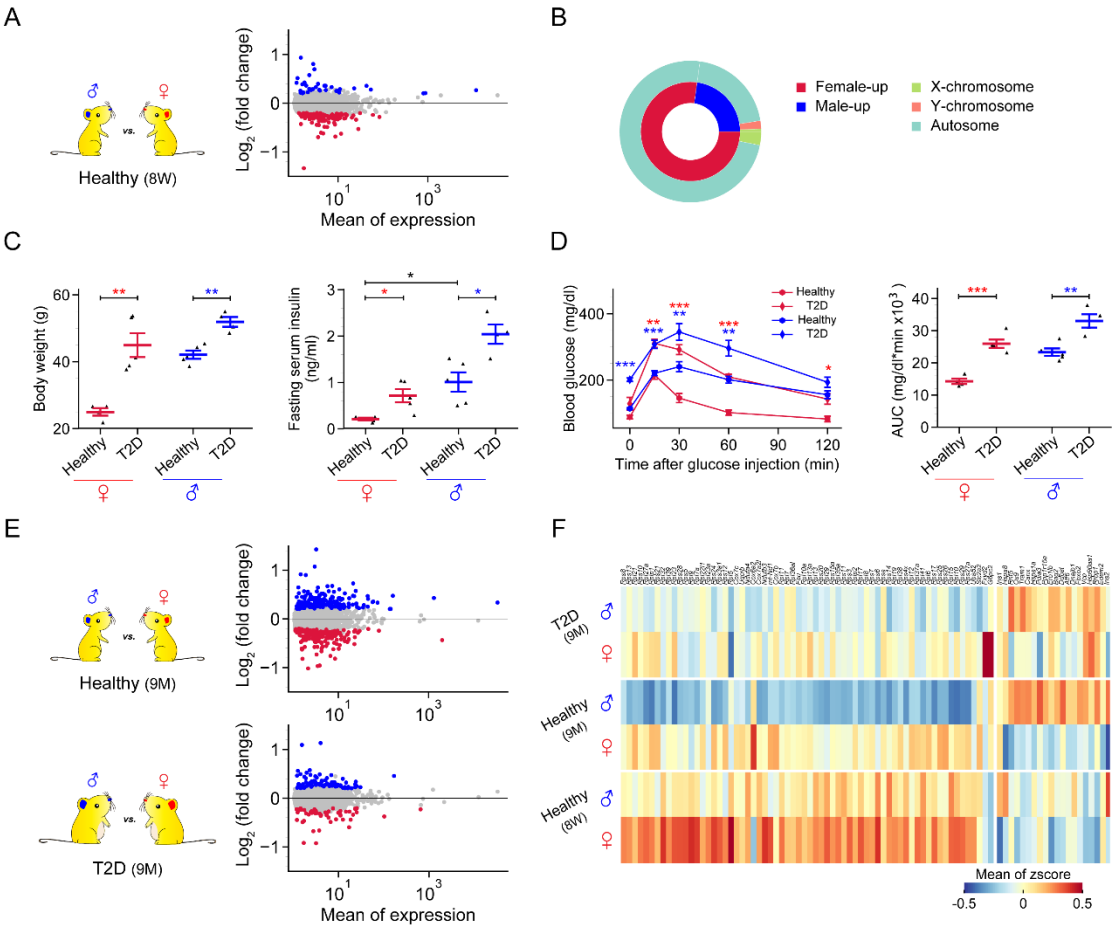

bioRxiv preprint doi: https://doi.org/10.1101/2020.09.22.307421; this version posted September 22, 2020. The copyright holder for this preprint (which was not certified by peer review) is the author/funder. All rights reserved. No reuse allowed without permission.

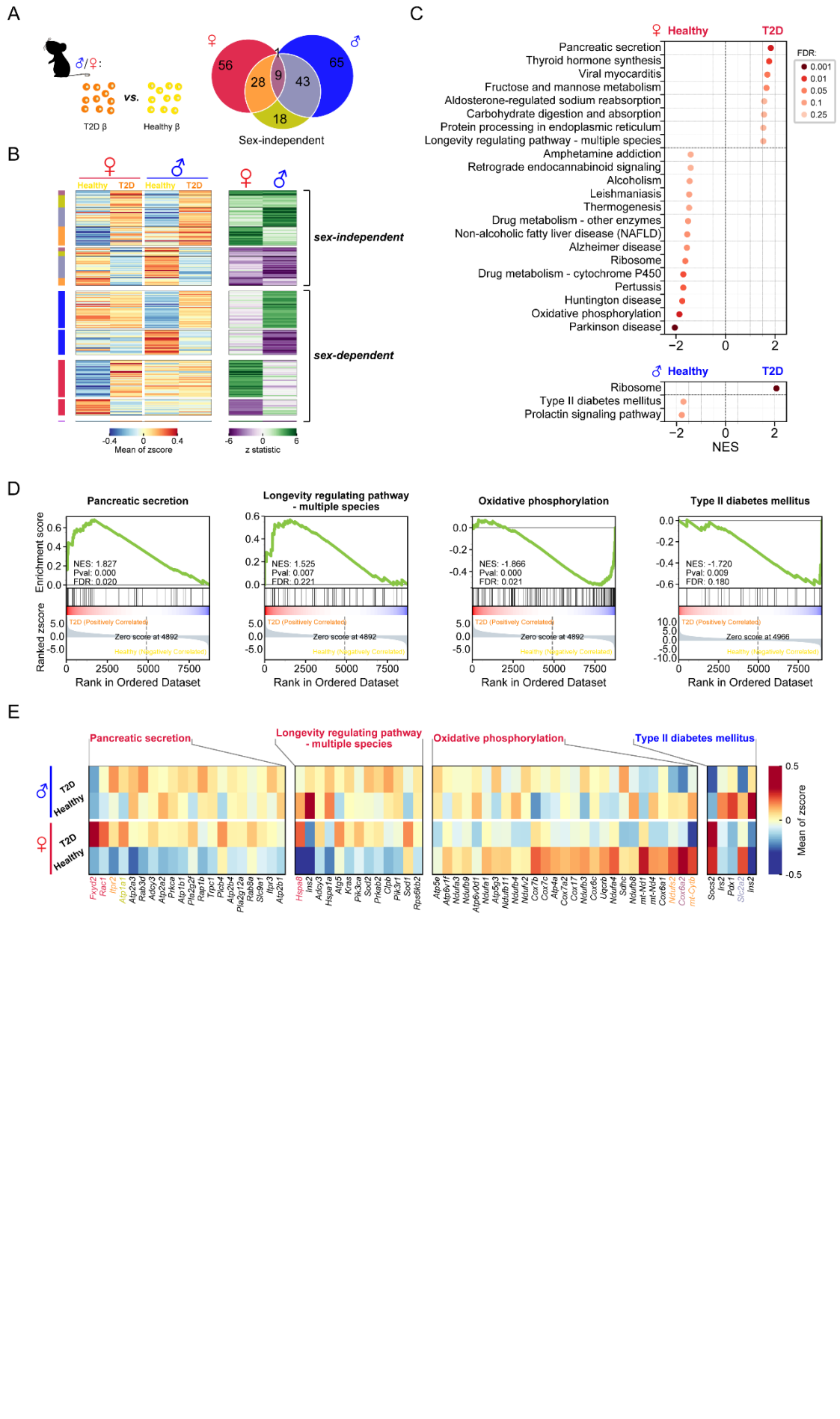

bioRxiv preprint doi: https://doi.org/10.1101/2020.09.22.307421; this version posted September 22, 2020. The copyright holder for this preprint (which was not certified by peer review) is the author/funder. All rights reserved. No reuse allowed without permission.

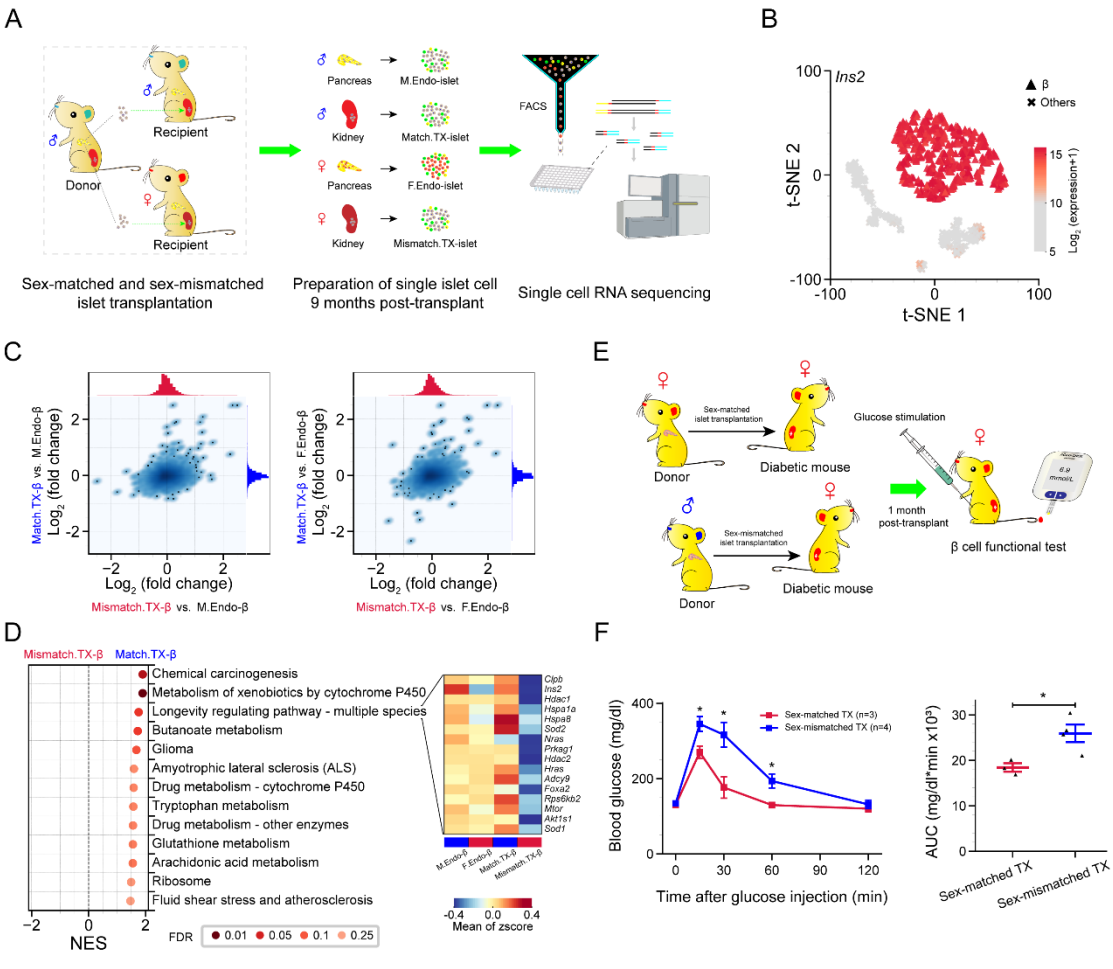

Strain	Age	Condition	Theoretic number of cells		Total
C57BL/6J	6-8 weeks	Healthy	Male:1056	Female:768	1824
C57BL/6J	9 months	Diabetic (HFD)	Male:576	Female:576	1152
C57BL/6J	9 months	Healthy(ND)	Male:576	Female:480	1056
ICR	11 months	Endogenous	Male:384	Female:384	768
ICR	11 months	Transplanted	Male:288	Female:384	672
Total				5472	

bioRxiv preprint doi: https://doi.org/10.1101/2020.09.22.307421; this version posted September 22, 2020. The copyright holder for this preprint (which was not certified by peer review) is the author/funder. All rights reserved. No reuse allowed without permission.

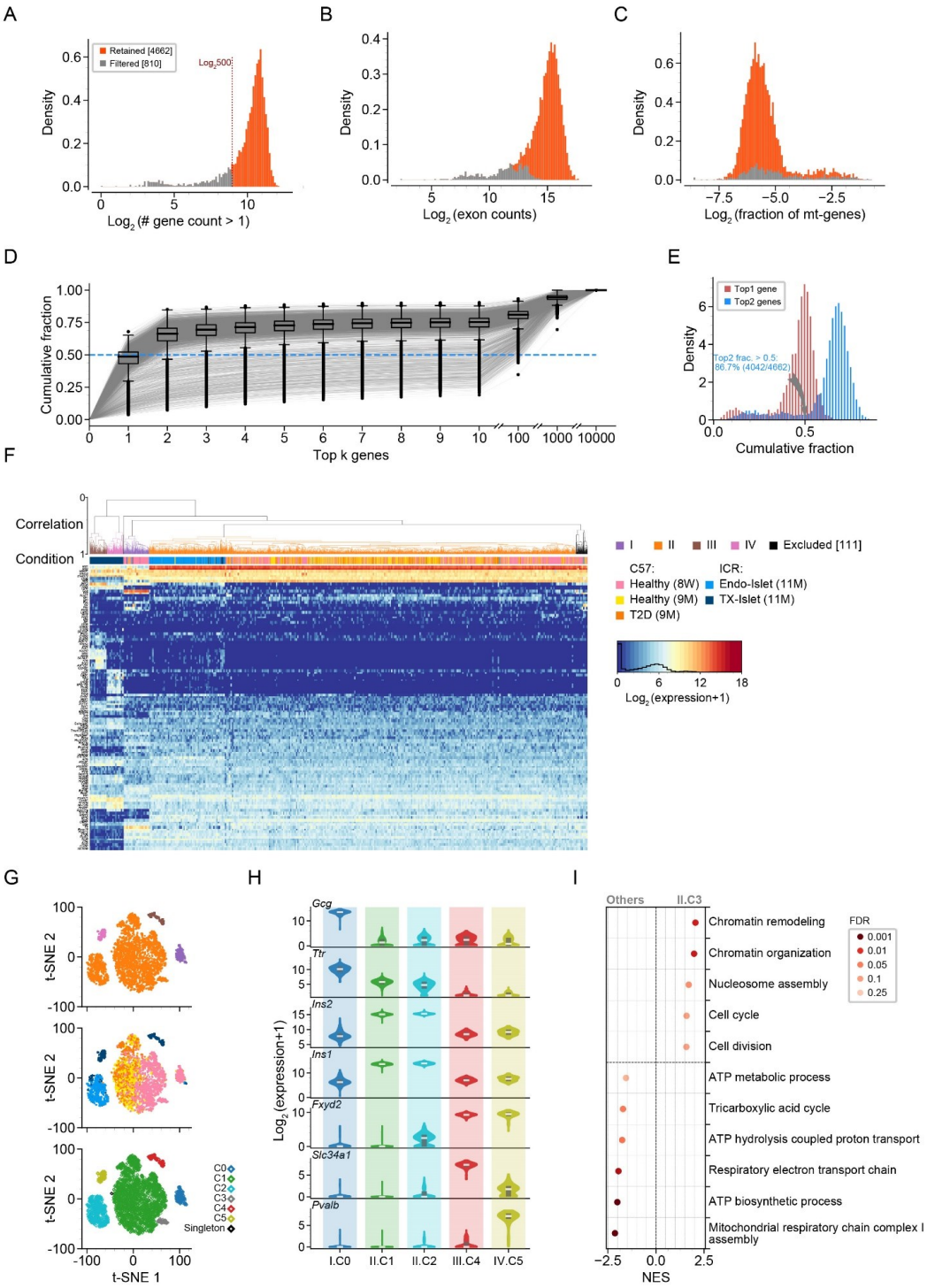

bioRxiv preprint doi: https://doi.org/10.1101/2020.09.22.307421; this version posted September 22, 2020. The copyright holder for this preprint (which was not certified by peer review) is the author/funder. All rights reserved. No reuse allowed without permission.

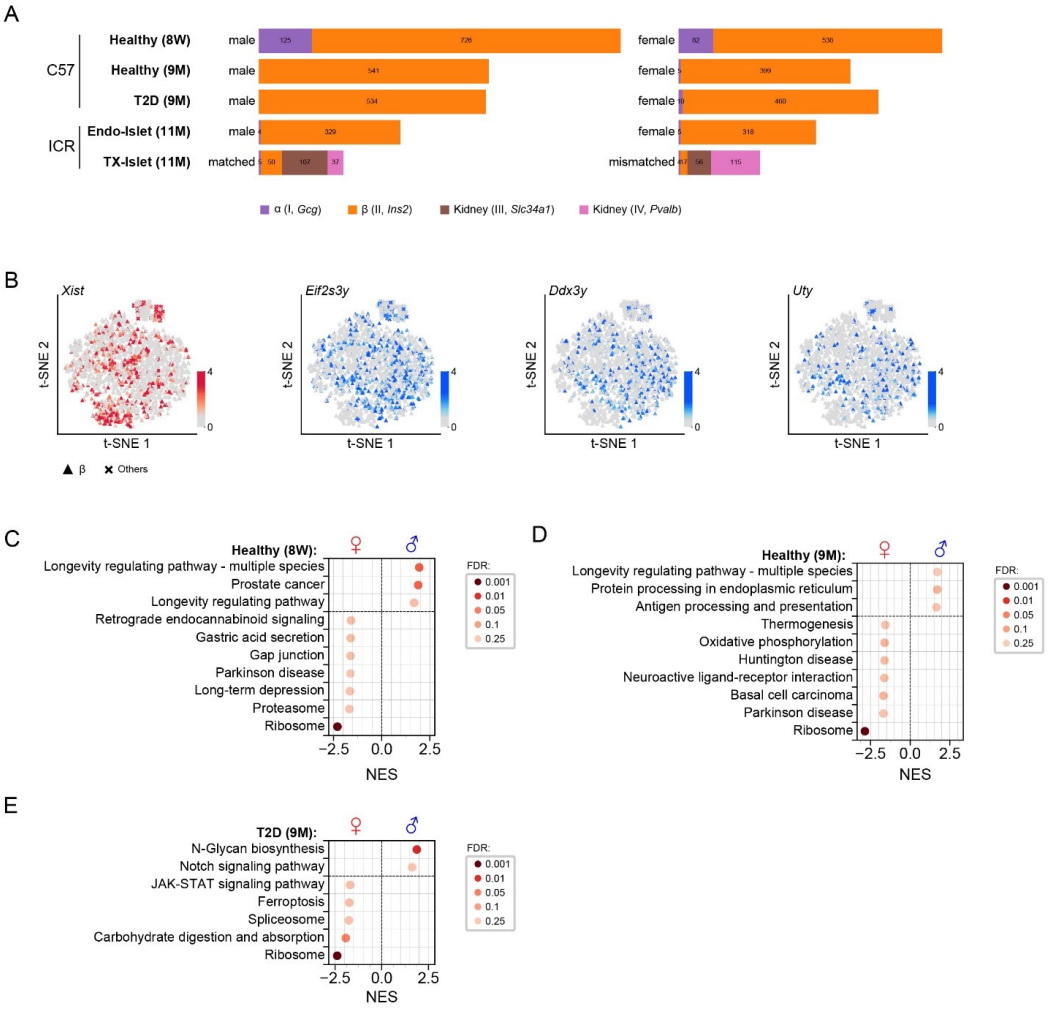

bioRxiv preprint doi: https://doi.org/10.1101/2020.09.22.307421; this version posted September 22, 2020. The copyright holder for this preprint (which was not certified by peer review) is the author/funder. All rights reserved. No reuse allowed without permission.

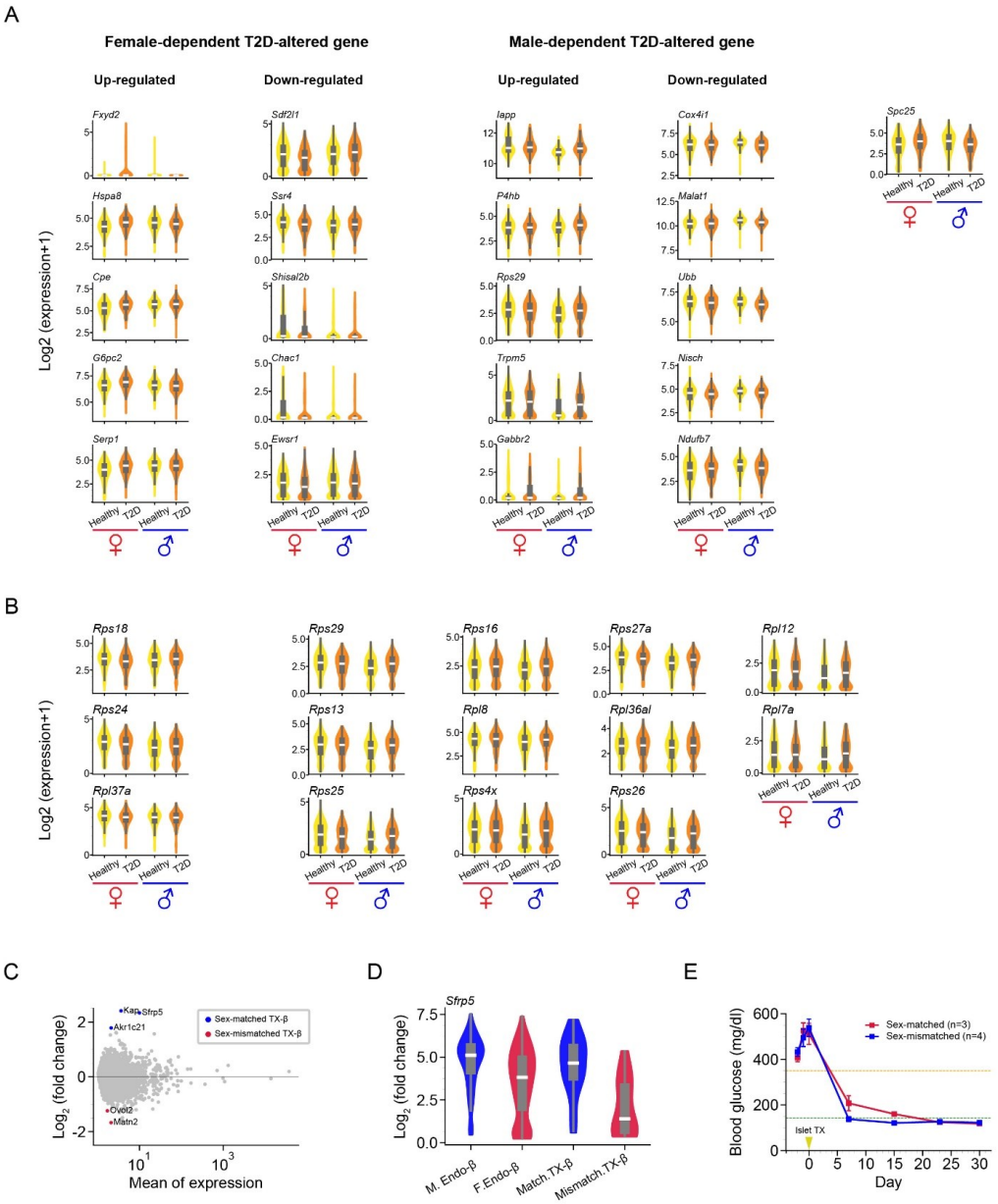

424

425

426

427

428

429

bioRxiv preprint doi: https://doi.org/10.1101/2020.09.22.307421; this version posted September 22, 2020. The copyright holder for this preprint (which was not certified by peer review) is the author/funder. All rights reserved. No reuse allowed without permission.

Discussion

According to previously published work, it has been well recognized that sexual dimorphism exists in many organs or systems, such as heart, kidney and immune responses [29-31]. What's more, a recent study in humans has shown that sexual dimorphism not only exhibits in neuron cells, but also is associated with susceptibility of mental diseases [32]. Herein, T2D is a complex metabolic disorder characterized with islet β cell failure and impacted by sex. Sex differences in islet β cell physiological function and diabetes prevalence have been recognized, but still need to be better understood. To decipher the sexually dimorphic T2D pathogenesis, we used scRNA-seq to comprehensively measure the transcriptomes of healthy and diabetic β cells from mice of both sexes. We identified abundant genes have significantly sex-biased expression in β cells of both healthy and T2D mouse. Besides, we found longevity regulating pathway was male specific enriched in healthy β cells. Furthermore, we identified 122 sex-dependent T2D altered genes in mouse, suggesting important differences in the molecular mechanisms of diabetes pathogenesis between males and females in mouse T2D model. Collectively, these results provided innovative sex-specific targets for future studies on the precision treatment of T2D.

In current clinical trials of islet transplantation, sex matching between donor and recipient has not been stressed. Based on the recognition of sex differences in the transcriptome of β cells, we concluded that sex as a crucial biological variance should be emphasized in the treatment of diabetes. And this conclusion was further supported by the sex-matched and sex-mismatched islet transplantation in mice. Compared with the sex-mismatched group, the β cells of transplants in the sex-matched group showed significant enrichment of the longevity regulating pathway (consistent with the results of Figure S2C and S2D) and glucose tolerance notably improved. For better curative effect, our result raised the necessity for sex-matched islet transplantation, and even for sex-matched stem cell-based cell replacement therapy for diabetes treatment.

bioRxiv preprint doi: https://doi.org/10.1101/2020.09.22.307421; this version posted September 22, 2020. The copyright holder for this preprint (which was not certified by peer review) is the author/funder. All rights reserved. No reuse allowed without permission.

Beyond the islet β cells focused in this study, sex differences of T2D susceptibility were also associated with sex steroid hormones. It has been found that endogenous estrogens are protective against T2D in females and the risk of T2D increases following menopause [33, 34]. Estrogen not only improves islet β cell function and survival [35], but also stimulates the secretion of GLP-1 by both islet α cells and intestine L cells to maintain glucose homeostasis [36]. Along with that, deficiency of the male sex hormone, testosterone, increases the T2D risk in male [37, 38]. Furthermore, a recent report revealed that testosterone improves insulin secretion through androgen receptor on male islet β cells in both mouse and human [12]. Taken together, sex differences in both islet β cells and sex steroid hormones need to be highlighted in the development of sex-specific precision medicine.

Materials and methods

Animals and high fat diet induced diabetic mice

All experiments were performed in accordance with the University of Health Guide for the Care and Use of Laboratory Animals and were approved by the Biological Research Ethics Committee of Tongji University. We housed all the mice under the specific pathogen free grade environment of animal facility at Tongji University, Shanghai, China. Adult male and female mice (6-8 weeks old) were purchased from Shanghai Slac Laboratory Animal. To induce mouse T2D model, male and female C57BL/6J mice (n=5 per sex) were fed with high-fat diet from 8-week-old to 9-month-old as a high-fat-diet (HFD) group, and equal number of male and female mice were fed up with normal diet (ND) in an age-matched way to a control potential confounding factor, age.

Islet transplantation

Islets were isolated from 6-8 weeks old male ICR mice (n=20), and the detailed process of islet isolation was as previous description [39]. Similar size islets were handpicked after purification under a stereomicroscope, and 3 age-matched healthy male and 3

bioRxiv preprint doi: https://doi.org/10.1101/2020.09.22.307421; this version posted September 22, 2020. The copyright holder for this preprint (which was not certified by peer review) is the author/funder. All rights reserved. No reuse allowed without permission.

485 female ICR mice were selected as a recipient with about 300-400 islets were
486 transplanted under the kidney capsule. About 9 months later, transplanted islets were
487 dissected and scraped from the kidney capsule, and the pellet was collected and
488 dissociated into a single cell for scRNA-seq in two batches. At the same time, the
489 endogenous islets of recipient mice were also isolated and dissociated into a single cell
490 for scRNA-seq. Diabetic mice and islet transplantation were both performed as
491 previous description [39]. Adult male and female C57BL/6J mice were selected as islet
492 donor, and age-matched female C57BL/6J mice were chosen as recipient. C57BL/6J
493 mice were injected with STZ at the dose of 170 mg/kg after 6 hours of fast. Mice that
494 exhibited non-fasting hyperglycemia (>350 mg/kg) with 3 consecutive detection were
495 regarded as diabetic mice for islet transplantation. Each diabetic mouse was
496 transplanted with about 350 islets, and mice that non-fasting blood glucose (<144
497 mg/kg) recover normal were selected for physiological experiments 1 month post-
498 transplant.
499
500 **Preparation of single islet cells**
501 Mouse islets were isolated from either 6-8 weeks old male or female C57BL/6J and
502 ICR mice. For islets isolation, 0.5 mg/mL collagenase P (Roche) was poured into
503 pancreas by perfusion of the common bile duct. After digestion, islets were purified
504 through Histopaque (Sigma) gradient centrifugation. The Histopaque buffer was made
505 with mixing Histopaque-10771 and Histopaque-11191 together as the ratio of 5:6.
506 Purified islets were dissociated into single cells as follows: washed the islets with cold
507 PBS at least two times, spun at 1000 rpm for 2 minutes, then replace PBS with 1mL
508 TrypLE Express (Gibco) and incubated at 37˚C for 10-15 minutes with pipetting cell
509 pellet by using P1000 pipette gently. Stop the reaction with low glucose DMEM
510 (containing 10% FBS, 1% HEPES, 1% PenStrep), and centrifuged cells at 4˚C, 1000
511 rpm for 2 min. Then washed the cell pellet with cold PBS for 1 time, and the
512 resuspended cells in PBS (containing 0.5%BSA) was filtered with a 40-micrometer

bioRxiv preprint doi: https://doi.org/10.1101/2020.09.22.307421; this version posted September 22, 2020. The copyright holder for this preprint (which was not certified by peer review) is the author/funder. All rights reserved. No reuse allowed without permission.

strainer to get single cell suspension. To obtain live single cell, Calcein Blue, AM (Invitrogen) was used to measure the viability of cell and high viability single cell was sorted by using BD FACS Aria II flow cytometry. Single islet cell was sorted into 96-well plates containing lysis buffer.

Library construction and NGS sequencing

Single-cell RNA-seq libraries were constructed according to Smart-seq2 protocol except that oligod (T) primers comprising 16bp cell barcode sequence and 9bp molecular barcode sequence were used to allow sample pooling and molecular counting. In addition, part of Truseq read2 sequence was used to replace ISPCR sequence in the oligod (T) primer thus to be compatible with Illumina sequence platform. Cells in lysis buffer were denatured, reverse transcribed in the presence of template switching oligos and pre-amplified by adding both ISPCR and ISPCR-read2 primers with 24 PCR cycles. cDNA of cells with different barcodes were then pooled together and were purified using 0.8x AMPure XP beads. Homemade Tn5 enzyme was used to tagment cDNA. Final amplification was processed using P7-index primers (Truseq) and P5-index primers (Nextera). Sequencing libraries were purified twice using 0.6x AMPure XP beads and once with 1x AMPure XP beads, and were sequenced on Illumina HiSeq X10 platform with default parameters. Primer and adaptor sequences were all listed in supplementary Table S3 (information of barcode).

Physiology experiment

For intraperitoneal injection glucose tolerance test, normal diet and high-fat diet feeding mice fasted for 16 hours. 1 g/Kg body weight of glucose was intraperitoneally injected, and blood glucose was measured at time point of 0 min, 15 min, 30 min, 60 min, 120 min after glucose injection using glucometer (ACCU-CHEK). Blood samples were collected from the mice that fasted for 6 hours, to measure the insulin level by using Mouse Ultrasensitive Insulin ELISA Kit (ALPOC). For oral glucose tolerance test,

bioRxiv preprint doi: https://doi.org/10.1101/2020.09.22.307421; this version posted September 22, 2020. The copyright holder for this preprint (which was not certified by peer review) is the author/funder. All rights reserved. No reuse allowed without permission.

mice were fasted for 6 hours, and glucose was gavaged at a dose of 2 g/Kg. Tail blood was collected for blood glucose detection, at time point of 0 min, 15 min, 30 min, 60 min, 120 min, using glucometer (ACCU-CHEK).

Quantification and statistical analysis

Preprocessing before normalization

Reads were stored in paired-end fastq format. Reads of one end of fragment contain cell barcode and UMI information which was subsequently extracted and added to the name of corresponding reads of the other end in fastq file containing molecular sequence. That barcode/UMI information was in fastq-R2 files. Next, the generated single-end fastq files were cleaned by Trim Galore! http://www.bioinformatics.babraham.ac.uk/projects/trim_galore/ with the parameter --length 30.

Then, the FastQC https://www.bioinformatics.babraham.ac.uk/projects/fastqc/ was applied to check reads quality before subsequent alignment on mm9 genome using STAR [40]. The parameters of STAR software were --AlignEndsType EndToEnd --out FileterMismatchNoverReadLmax 0.04 --outSAMattrIHstart 0 --outSAMmultNmax 1 --outFilterMultimapNmax 1. GTF file of mm9 reference genome was derived from the RefSeq gene annotation [41] file downloaded from UCSC genome browser database , http://genome.ucsc.edu/cgi-bin/hgGateway?db=mm9. After alignment, SAM files underwent demultiplexing by Catadapt https://github.com/marcelm/cutadapt/releases with --overlap 16 –no-indels --match-read-wildcards parameters; reads were removed if they were assigned to more than one cells. Then, we removed PCR duplicates by UMI-tools [42]. Next, featureCounts [43] was utilized to quantify gene expression levels according to the above mentioned GTF file. Once the expression profiles were generated, cells with fewer than 500 expressed genes (UMI count > 1) were considered low-quality and were removed (Figure S1). The fraction of transcripts from mitochondrial genes in each single cell was investigated as it was used as an indicator

bioRxiv preprint doi: https://doi.org/10.1101/2020.09.22.307421; this version posted September 22, 2020. The copyright holder for this preprint (which was not certified by peer review) is the author/funder. All rights reserved. No reuse allowed without permission.

for general quality control. Part of our ICR cells had high transcripts fraction of mitochondrial genes, which can be accounted for that kidney cells intrinsically express high-level mitochondrial genes [44]. So we kept those cells for analysis because our transplantation cells were under renal capsule and either kidney cells or affected transplant cells may well be introduced in our data. Next, only genes expressed (UMI count > 1) in 5 or more cells were used for further analysis. Eventually, there are 14,152 genes and 4662 cells retained in mouse scRNA-seq data. The sample information of the Illumina high-throughput sequencing data is listed as following table.

Normalization

Here we used an adjusted count per million (CPM) normalization method, named adjCPM. The CPM method assumes that the total molecule reads are equal among cells. Similarly, our adjCPM method has an assumption except excluding a few genes in calculating the total number of molecular reads of each cell. It is based on the observation that sometimes a few top expressed genes can possess more than 50% total UMI count (Figure S1). These genes were selected as union set of the top 2 expressed genes of single cells in which the sum of the corresponding top 2 genes' UMI counts is beyond 50% of the total count of the cell. Specifically, we obtained 9 genes (*Gcg*, *Ins1*, *Ins2*, *Malat1*, *Ppy*, *Pyy*, *Rn45s*, *Ttr*, *mt-Rnr2*) and they were excluded when calculating the total count of each cell. It is well known that the scRNA-seq experiments are affected by drop-out events especially for UMI method. Here, we also observed that many genes have zero expression value because of insufficient detection power or intrinsically under-expressed. To address this issue, SAVER [45] was applied to recover gene expression in the entire matrix.

Cell type identification

Since cell type identification is critical for the rest analysis, two steps were carried out to robustly define the cell type. Firstly, we selected the top 10 expressed genes of each

bioRxiv preprint doi: https://doi.org/10.1101/2020.09.22.307421; this version posted September 22, 2020. The copyright holder for this preprint (which was not certified by peer review) is the author/funder. All rights reserved. No reuse allowed without permission.

cell, resulting in a total of 118 genes to perform the subsequent hieratical clustering analysis. Accordingly, we primarily assigned 4 clusters of single cells after removing 111 cells which had ulterior distance in clustering dendrogram and annotated each cluster based on marker gene expression (Figure S1).

Secondly, by a lowess regression between the Log2 mean and Log2 coefficient of variance of each gene's normalized UMI count across all single cells, we selected 3000 genes according to the residue of lowess regression as hypervariable genes (HVGs). Next, principal component analysis (PCA) was applied to the Log2 transformed normalized expression of these HVGs using *sklearn* [46] after centering and scaling, and top 25 PCs were selected based on the statistical significance of the fraction of total variance explained by each of them, which was estimated using jackstraw [47]. We used the top 25 PCs as input for subsequent t-Distributed Stochastic Neighbor Embedding (t-SNE) analysis. To have a stable t-SNE visualization, we tried a lot of combinations of parameters (perplexing [10, 15, 20, 25, 30], early exaggeration [12, 15, 20], learning rate [200, 300, 400, 500, 600, 800] and 50 random seeds) using *sklearn* [46], and found they generally gave very similar results. We finally chose perplexing:15, early exaggeration:12, learning rate:500 to generate the t-SNE plots shown in the figures. Next, Density-based spatial clustering algorithm, DBSCAN [48] with parameters eps=5 and MinPts=5 was applied on the resulting two-dimensional t-SNE map to group the single cells into cliques (Figure S1G). After removing singletons, we examined each single cell clique in order of clique size with following criteria: 1. only cells with consistent cluster/clique labels generated by hierarchical clustering using the top expressed genes and by DBSCAN were retained; 2. differential expression analysis of single cells in clique 3 (C3) compared the single cells in other cliques demonstrated that the single cells in C3 should be excluded because they highly expressed cell cycle related genes (Figure S1I). Finally, we kept 4467 high-quality mouse single cells for downstream analysis, and the cell type labels were inferred from the marker genes highly expressed in each single cell clique (Figure S1H).

bioRxiv preprint doi: https://doi.org/10.1101/2020.09.22.307421; this version posted September 22, 2020. The copyright holder for this preprint (which was not certified by peer review) is the author/funder. All rights reserved. No reuse allowed without permission.

Differential expression analysis and gene set enrichment analysis

MAST [17] was used to perform differential expression analysis between male and female or between T2D and healthy scRNA-seq profiles of β cells. Cellular detection rate (CDR, which means the number of genes detected in each single cell) was controlled as a covariate while estimating treatment effects. Significantly regulated genes were identified by using false discovery rate <=0.05 as cutoff. For identification of functional pathways enriched in the detected differentially expressed genes between different sexes or between T2D and healthy conditions in our scRNA-seq data, we performed gene set enrichment analysis (GSEA) [19] on genes ranked based on their z-statistics, which were derived by mapping their MAST p-values to the standard normal distribution and using the sign of the Log2(fold change) of their expression values to represent the direction of regulation. Technically, the z-statistic of each gene was calculated as:

$$\mathrm{qnorm}(p) \times \mathrm{sign}(\mathrm{lfc})$$

where p and lfc are p-value and Log2(fold change) of this gene obtained from MAST output, qnorm is the standard normal quantile function and sign is the signum function. KEGG pathways [49] were used as input gene sets for GSEA, and fdr cutoff of 0.25 was used to select statistically significant pathways.

Accession number

Raw data (Fastq files) for single pancreatic β cell RNA-seq in this study have been submitted to National Omics Data Encyclopedia (NODE) with accession number OEP000892.

Authors' contributions

GL and WL designed the research; GL, YL, TZ, ML performed the research and data analysis; GL, SL, SL and MX performed animal experiments; GL, TZ, SL prepared

bioRxiv preprint doi: https://doi.org/10.1101/2020.09.22.307421; this version posted September 22, 2020. The copyright holder for this preprint (which was not certified by peer review) is the author/funder. All rights reserved. No reuse allowed without permission.

653 samples for single-cell RNA sequencing; WL, ZS and WS supervised all aspects of the
654 study; GL and WL wrote the manuscript.
655

656 ## Competing interests

657 The authors have declared no competing interests.
658

659 ## Acknowledgments

660 This work was supported by the National Key Research and Development Program of
661 China (2016YFA0102200, 2017YFA0106500, 2018YFA0107102) awarded to WL;
662 and the National Key Research and Development Program of China
663 (2018YFA0107602) awarded to ZS; WS is supported by the Funding Project of
664 National Key Research and Development Program of China (2018YFD0900604),
665 Natural Science Foundation of China (41676119, 41476120) and start-up fund from
666 Ocean University of China.
667
668

bioRxiv preprint doi: https://doi.org/10.1101/2020.09.22.307421; this version posted September 22, 2020. The copyright holder for this preprint (which was not certified by peer review) is the author/funder. All rights reserved. No reuse allowed without permission.

669 # References

670 [1] Zucker I, Beery AK. Males still dominate animal studies. Nature 2010;465:690.

671 [2] Mauvais-Jarvis F, Arnold AP, Reue K. A guide for the design of pre-clinical studies
672 on sex differences in metabolism. Cell Metabolism 2017;25:1216-30.

673 [3] Clayton JA, Collins FS. Policy: NIH to balance sex in cell and animal studies.
674 Nature 2014;509:282-3.

675 [4] Zhang Q, Bengtsson M, Partridge C, Salehi A, Braun M, Cox R, et al. R-type
676 Ca(2+)-channel-evoked CICR regulates glucose-induced somatostatin secretion. Nat
677 Cell Biol 2007;9:453-60.

678 [5] Holzer P, Reichmann F, Farzi A. Neuropeptide Y, peptide YY and pancreatic
679 polypeptide in the gut-brain axis. Neuropeptides 2012;46:261-74.

680 [6] Vital P, Larrieta E, Hiriart M. Sexual dimorphism in insulin sensitivity and
681 susceptibility to develop diabetes in rats. J Endocrinol 2006;190:425-32.

682 [7] Yokomizo H, Inoguchi T, Sonoda N, Sakaki Y, Maeda Y, Inoue T, et al. Maternal
683 high-fat diet induces insulin resistance and deterioration of pancreatic beta-cell function
684 in adult offspring with sex differences in mice. Am J Physiol Endocrinol Metab
685 2014;306:E1163-75.

686 [8] Logue J, Walker JJ, Colhoun HM, Leese GP, Lindsay RS, McKnight JA, et al. Do
687 men develop type 2 diabetes at lower body mass indices than women? Diabetologia
688 2011;54:3003-6.

689 [9] Wandell PE, Carlsson AC. Gender differences and time trends in incidence and
690 prevalence of type 2 diabetes in Sweden--a model explaining the diabetes epidemic
691 worldwide today? Diabetes Res Clin Pract 2014;106:e90-2.

692 [10] Kautzky-Willer A, Harreiter J, Pacini G. Sex and gender differences in risk,
693 pathophysiology and complications of Type 2 Diabetes Mellitus. Endocr Rev
694 2016;37:278-316.

695 [11] Hall E, Volkov P, Dayeh T, Esguerra JL, Salo S, Eliasson L, et al. Sex differences
696 in the genome-wide DNA methylation pattern and impact on gene expression,

bioRxiv preprint doi: https://doi.org/10.1101/2020.09.22.307421; this version posted September 22, 2020. The copyright holder for this preprint (which was not certified by peer review) is the author/funder. All rights reserved. No reuse allowed without permission.

697 microRNA levels and insulin secretion in human pancreatic islets. Genome Biol
698 2014;15:522.
699 [12] Navarro G, Xu W, Jacobson DA, Wicksteed B, Allard C, Zhang G, et al.
700 Extranuclear actions of the androgen receptor enhance glucose-stimulated insulin
701 secretion in the male. Cell Metab 2016;23:837-51.
702 [13] Small KS, Todorcevic M, Civelek M, El-Sayed Moustafa JS, Wang X, Simon MM,
703 et al. Regulatory variants at KLF14 influence type 2 diabetes risk via a female-specific
704 effect on adipocyte size and body composition. Nat Genet 2018;50:572-80.
705 [14] Xin Y, Kim J, Okamoto H, Ni M, Wei Y, Adler C, et al. RNA sequencing of single
706 human islet cells reveals Type 2 Diabetes genes. Cell Metab 2016;24:608-15.
707 [15] Lawlor N, George J, Bolisetty M, Kursawe R, Sun L, Sivakamasundari V, et al.
708 Single-cell transcriptomes identify human islet cell signatures and reveal cell-type-
709 specific expression changes in type 2 diabetes. Genome Res 2017;27:208-22.
710 [16] Segerstolpe A, Palasantza A, Eliasson P, Andersson EM, Andreasson AC, Sun X,
711 et al. Single-cell transcriptome profiling of human pancreatic islets in health and Type
712 2 Diabetes. Cell Metab 2016;24:593-607.
713 [17] Finak G, McDavid A, Yajima M, Deng J, Gersuk V, Shalek AK, et al. MAST: a
714 flexible statistical framework for assessing transcriptional changes and characterizing
715 heterogeneity in single-cell RNA sequencing data. Genome Biol 2015;16:278.
716 [18] Sone H, Kagawa Y. Pancreatic beta cell senescence contributes to the pathogenesis
717 of type 2 diabetes in high-fat diet-induced diabetic mice. Diabetologia 2005;48:58-67.
718 [19] Subramanian A, Tamayo P, Mootha VK, Mukherjee S, Ebert BL, Gillette MA, et
719 al. Gene set enrichment analysis: a knowledge-based approach for interpreting genome-
720 wide expression profiles. Proc Natl Acad Sci USA 2005;102.
721 [20] Arystarkhova E, Liu YB, Salazar C, Stanojevic V, Clifford RJ, Kaplan JH, et al.
722 Hyperplasia of pancreatic beta cells and improved glucose tolerance in mice deficient
723 in the FXYD2 subunit of Na,K-ATPase. Journal of Biological Chemistry
724 2013;288:7077-85.

bioRxiv preprint doi: https://doi.org/10.1101/2020.09.22.307421; this version posted September 22, 2020. The copyright holder for this preprint (which was not certified by peer review) is the author/funder. All rights reserved. No reuse allowed without permission.

[21] Alam M-u, Harken JA, Knorn A-M, Elford AR, Wigmore K, Ohashi PS, et al. Transgenic expression of Hsc70 in pancreatic islets enhances autoimmune diabetes in response to β cell damage. The Journal of Immunology 2009;183:5728-37.

[22] Davidson HW, Hutton JC. The insulin-secretory-granule carboxypeptidase H. Purification and demonstration of involvement in proinsulin processing. Biochemical Journal 1987;245:575-82.

[23] Pound LD, Oeser JK, O'Brien TP, Wang Y, Faulman CJ, Dadi PK, et al. G6PC2: a negative regulator of basal glucose-stimulated insulin secretion. Diabetes 2013;62:1547-56.

[24] Cooper GJ, Willis AC, Clark A, Turner RC, Sim RB, Reid KB. Purification and characterization of a peptide from amyloid-rich pancreases of type 2 diabetic patients. Proceedings of the National Academy of Sciences 1987;84:8628.

[25] Jang I, Pottekat A, Poothong J, Yong J, Lagunas-Acosta J, Charbono A, et al. PDIA1/P4HB is required for efficient proinsulin maturation and ss cell health in response to diet induced obesity. Elife 2019;8.

[26] Larsson MH, Hakansson P, Jansen FP, Magnell K, Brodin P. Ablation of TRPM5 in mice results in reduced body weight gain and improved glucose tolerance and protects from excessive consumption of sweet palatable food when fed high caloric diets. PLoS One 2015;10:e0138373.

[27] Ouchi N, Higuchi A, Ohashi K, Oshima Y, Gokce N, Shibata R, et al. Sfrp5 Is an anti-inflammatory adipokine that modulates metabolic dysfunction in obesity. Science 2010;329:454-7.

[28] Carstensen-Kirberg M, Kannenberg JM, Huth C, Meisinger C, Koenig W, Heier M, et al. Inverse associations between serum levels of secreted frizzled-related protein-5 (SFRP5) and multiple cardiometabolic risk factors: KORA F4 study. Cardiovasc Diabetol 2017;16:109.

bioRxiv preprint doi: https://doi.org/10.1101/2020.09.22.307421; this version posted September 22, 2020. The copyright holder for this preprint (which was not certified by peer review) is the author/funder. All rights reserved. No reuse allowed without permission.

751 [29] Skelly DA, Squiers GT, McLellan MA, Bolisetty MT, Robson P, Rosenthal NA, et
752 al. Single-cell transcriptional profiling reveals cellular diversity and
753 intercommunication in the mouse heart. Cell Rep 2018;22:600-10.
754 [30] Ransick A, Lindstrom NO, Liu J, Zhu Q, Guo JJ, Alvarado GF, et al. Single-cell
755 profiling reveals sex, lineage, and regional diversity in the mouse kidney. Dev Cell
756 2019;51:399-413 e7.
757 [31] Klein SL, Flanagan KL. Sex differences in immune responses. Nature Reviews
758 Immunology 2016;16:626-38.
759 [32] Lobentanzer S, Hanin G, Klein J, Soreq H. Integrative transcriptomics reveals
760 sexually dimorphic control of the cholinergic/neurokine interface in schizophrenia and
761 bipolar disorder. Cell Rep 2019;29:764-77 e5.
762 [33] Mauvais-Jarvis F, Clegg DJ, Hevener AL. The role of estrogens in control of
763 energy balance and glucose homeostasis. Endocrine reviews 2013;34:309-38.
764 [34] Tramunt B, Smati S, Grandgeorge N, Lenfant F, Arnal J-F, Montagner A, et al. Sex
765 differences in metabolic regulation and diabetes susceptibility. Diabetologia
766 2020;63:453-61.
767 [35] Tiano JP, Mauvais-Jarvis F. Importance of oestrogen receptors to preserve
768 functional β-cell mass in diabetes. Nature reviews. Endocrinology 2012;8:342-51.
769 [36] Handgraaf S, Dusaulcy R, Visentin F, Philippe J, Gosmain Y. 17-β Estradiol
770 regulates proglucagon-derived peptide secretion in mouse and human α- and L cells.
771 JCI insight 2018;3:e98569.
772 [37] Basaria S, Muller DC, Carducci MA, Egan J, Dobs AS. Hyperglycemia and insulin
773 resistance in men with prostate carcinoma who receive androgen-deprivation therapy.
774 Cancer 2006;106:581-8.
775 [38] Mauvais-Jarvis F. Estrogen and androgen receptors: regulators of fuel homeostasis
776 and emerging targets for diabetes and obesity. Trends Endocrinol Metab 2011;22:24-
777 33.

bioRxiv preprint doi: https://doi.org/10.1101/2020.09.22.307421; this version posted September 22, 2020. The copyright holder for this preprint (which was not certified by peer review) is the author/funder. All rights reserved. No reuse allowed without permission.

778 [39] Zmuda EJ, Powell CA, Hai T. A method for murine islet isolation and subcapsular
779 kidney transplantation. J Vis Exp 2011.
780 [40] Dobin A, Davis CA, Schlesinger F, Drenkow J, Zaleski C, Jha S, et al. STAR:
781 ultrafast universal RNA-seq aligner. Bioinformatics (Oxford, England) 2013;29:15-21.
782 [41] Pruitt KD, Tatusova T, Maglott DR. NCBI Reference Sequence (RefSeq): a curated
783 non-redundant sequence database of genomes, transcripts and proteins. Nucleic Acids
784 Research 2005;33:D501-D4.
785 [42] Smith T, Heger A, Sudbery I. UMI-tools: modeling sequencing errors in Unique
786 Molecular Identifiers to improve quantification accuracy. Genome Res 2017;27:491-9.
787 [43] Liao Y, Smyth GK, Shi W. featureCounts: an efficient general purpose program for
788 assigning sequence reads to genomic features. Bioinformatics 2014;30:923-30.
789 [44] Park J, Shrestha R, Qiu C, Kondo A, Huang S, Werth M, et al. Single-cell
790 transcriptomics of the mouse kidney reveals potential cellular targets of kidney disease.
791 Science 2018;360:758-63.
792 [45] Huang M, Wang J, Torre E, Dueck H, Shaffer S, Bonasio R, et al. SAVER: gene
793 expression recovery for single-cell RNA sequencing. Nat Methods 2018;15:539-42.
794 [46] Pedregosa F, Varoquaux G, Gramfort A, Michel V, Thirion B, Grisel O, et al. Scikit-
795 learn: machine learning in Python. Journal of Machine Learning Research
796 2011;12:2825-30.
797 [47] Chung NC, Storey JD. Statistical significance of variables driving systematic
798 variation in high-dimensional data. Bioinformatics (Oxford, England) 2015;31:545-54.
799 [48] Ester M, Kriegel HP, Sander J, Xu X (1996), 'A Density-Based Algorithm for
800 Discovering Clusters in Large Spatial Databases with Noise', *Proceedings of the Second*
801 *International Conference on Knowledge Discovery and Data Mining*, pp. 226-31.
802 [49] Kanehisa M, Goto S. KEGG: kyoto encyclopedia of genes and genomes. Nucleic
803 Acids Res 2000;28:27-30.
804
805

bioRxiv preprint doi: https://doi.org/10.1101/2020.09.22.307421; this version posted September 22, 2020. The copyright holder for this preprint (which was not certified by peer review) is the author/funder. All rights reserved. No reuse allowed without permission.

Figure legends

Figure 1 Identification of β cells from mouse islet cells

A. Schematic diagram for mouse single β cell RNA-seq data preparation and analysis. Mouse single living islet cells are labelled by Calcein Blue, AM, and collected through Fluorescence activated cell sorting (FACS). β cells are sorted out and divided into different groups according to donor conditions. 8W, 8-week-old; 9M, 9-month-old. **B.** t-SNE map of cells from mouse in different conditions. The cells from healthy and T2D mice are colored with different red-colored items. **C.** Mouse β cells are identified by highly expressed marker gene *Ins2*. **D.** Mouse β cells are colored by sex information. And the expression of β cell marker *Ins2* is significantly different between cells of males and females (K-S test) as shown in the box plot.

Figure 2 Sex-biased gene expression in β cells of healthy and T2D mice

A. Comparison between β cells of male and female 8-week-old (8W) C57 mice. In the MA plot, the sex-biased genes are highlighted by blue (male-biased) and red (female-biased) dots. See also Table S1. **B.** Nested pie chart depicting genomic location of sex-biased genes. **C.** Diabetes associated physiological phenotypes. Body weight, fasting insulin serum level are detected. The blue line represents the sample of male healthy (n=5) and male T2D (n=4); red line represents the sample of female healthy (n=4) and female T2D (n=5). Results are presented as mean ± SEM; * $p \leq 0.05$, ** $p \leq 0.01$, two sample t-test. **D.** Intraperitoneal injection glucose tolerance test with area under curve (AUC). Results are presented as mean±SEM;* $p \leq 0.05$, ** $p \leq 0.01$; *** $p \leq 0.001$. Red *, **, *** represent female T2D (n=5) versus female healthy (n=4) mice; blue *, **, *** represent male T2D (n=4) versus male healthy (n=5) mice, two sample t-test. **E.** Comparisons between male and female β cells of 9-month-old (9M) healthy and T2D mice. In the MA plots, sex-biased genes are highlighted by blue (male-biased) and red (female-biased) dots. See also Table S1. **F.** Heatmap of genes selected from sex-biased genes that overlapped with the leading-edge genes of GSEA. See also Table S1.

bioRxiv preprint doi: https://doi.org/10.1101/2020.09.22.307421; this version posted September 22, 2020. The copyright holder for this preprint (which was not certified by peer review) is the author/funder. All rights reserved. No reuse allowed without permission.

834 **Figure 3 T2D altered genes and pathways in mouse β cells**

835 **A.** Venn diagram depicting the definition of sex-independent and sex-dependent T2D
836 altered genes. See also Table S2. **B.** Heatmap of sex-dependent and sex-independent
837 T2D altered genes. The left heatmap shows the mean of z-score of expression across
838 cells in each group, and the right heatmap shows the z-statistics of these genes derived
839 by mapping their MAST p-values to the standard normal distribution. The signs indicate
840 the direction they are regulated in both sexes. **C.** Results of GSEA showing pathways
841 significantly enriched in the healthy group and the T2D group in male (labeled in blue)
842 and female (labeled in red). Pathways with NES>0 are enriched in T2D β cells and
843 pathways with NES<0 are enriched in healthy β cells. **D.** GSEA plots of pathways
844 involved in the onset of diabetes or the function of β cell. **E.** Heatmap of leading-edge
845 genes of the selected pathways. The sex-dependent T2D altered genes are highlighted
846 in corresponding colors.
847
848 **Figure 4 Comparison of sex-matched and sex-mismatched islet transplantation**
849 **A.** Schematic diagram of sex-matched and sex-mismatched islet transplantation for
850 scRNA-seq. Single islet cells are collected for scRNA-seq 9 months post-transplant.
851 M.Endo-islet, endogenous islets of male recipients; F.Endo-islet, endogenous islets of
852 female recipients; Match.TX-islet, transplanted islets in male recipients; Mismatch.TX-
853 islet, transplanted islets in female recipients. **B.** t-SNE map of endogenous and
854 transplanted islet cells in both sex-matched and sex-mismatched transplantation, and β
855 cells are identified by highly expressed *Ins2*. Details see also Figure S2A. **C.** Scatterplot
856 depicting correlation of Log2(fold change) generated by comparing β cells of TX-β
857 (sex-matched or sex-mismatched) and endo-β. M.Endo-β, endogenous β cells of male
858 recipients; F.Endo-β, endogenous β cells of female recipients; Match.TX-β, sex-
859 matched transplant-β cells in male recipients; Mismatch.TX-β, sex-mismatched
860 transplant-β cells in female recipients. **D.** Pathways enriched in sex-matched transplant-
861 β cells. Leading-edge genes of longevity regulating pathway are zoomed in with heat-

bioRxiv preprint doi: https://doi.org/10.1101/2020.09.22.307421; this version posted September 22, 2020. The copyright holder for this preprint (which was not certified by peer review) is the author/funder. All rights reserved. No reuse allowed without permission.

map. M.Endo-β, endogenous β cells of male recipients; F.Endo-β, endogenous β cells of female recipients; Match.TX-β, sex-matched transplant-β cells in male recipients; Mismatch.TX-β, sex-mismatched transplant-β cells in female recipients. **E.** Schematic diagram of sex-matched and sex-mismatched islet transplantation for β cell functional test in STZ induced diabetic mouse. **F.** Oral glucose tolerance test (OGTT) for mice after sex-matched (n=3 mice) and sex-mismatched (n=4 mice) islet transplantation and results are summarized by the area under curve (AUC). 2 g/Kg glucose is gavaged after 6 hours fasting, and blood glucose level is detected at 0, 15, 30, 60, 120 minutes after glucose gavage. Results are presented as mean±SEM; * $p \leq 0.05$, two sample t-test. TX, transplantation.

Table 1 The number of collected cells from mice in different conditions

Supplementary material

Figure S1 Data processing for the identification of β cell

A. Distribution of detected gene numbers (Log2 transformed). 810 out of 5472 cells are removed from further analysis due to number of genes with more than 1 UMI count less than 500. **B.** Distribution of total exon counts (Log2 transformed). The retained cells (shown in orange) have relatively higher exon counts. **C.** Distribution of UMI fractions of mitochondrial genes (Log2 transformed). The retained cells (shown in orange) have relatively lower UMI fractions of mitochondrial genes. **D.** Boxplot of fraction of UMI count of top k most expressed genes. The fraction is beyond 0.5 for most cells when k = 2 Each gray line represents a cell. **E.** Distribution of UMI count fraction of top 1 (shown in red) and top 2 (shown in blue) most expressed genes. In 86.7% of the mouse islet cells, the UMI count fraction of the top 2 most expressed genes are more than 0.5. The union of the top 2 most expressed genes from all these cells includes 9 genes (*Gcg*, *Ins1*, *Ins2*, *Malat1*, *Ppy*, *Pyy*, *Rn45s*, *Ttr*, *mt-Rnr2*), which are excluded while calculating total count for normalization using adjCPM method. **F.**

bioRxiv preprint doi: https://doi.org/10.1101/2020.09.22.307421; this version posted September 22, 2020. The copyright holder for this preprint (which was not certified by peer review) is the author/funder. All rights reserved. No reuse allowed without permission.

Hierarchical clustering for 4,662 mouse islet single cells. Using union of the top 10 expressed genes in all cells (total 141 genes) with "euclidean" metric and "complete" linkage and 110 cells are excluded. 8W, 8-week-old; 9M, 9-month-old; 11M, 11-month-old; Endo-islet, endogenous islets of recipients; TX-islet, transplanted islets in recipients. **G.** t-SNE map of retained cells. Cells are colored by the clustering result of the previous hierarchical clustering (up panel), conditions (middle panel) and clique labels from DBSCAN clustering (down panel), respectively. **H.** Violin plots of marker genes for C0, C1, C2, C4, C5 after filtering cells with inconsistent cluster labels given by previous hierarchical clustering. C1: *Ins2* (a known marker gene of β cells) highly expressing cells from mice of C57 strain (labeled as β cells); C2: *Ins2* highly expressing cells from 11-month-old mice of ICR strain (labeled as β cells); C0: *Gcg* (a known marker gene of α cells) highly expressing cells (labeled as α cells); C4 and C5: two groups of cells with high expression of *Slc34a1* and *Pvalb* (two known marker genes of kidney proximal tubule and distal convoluted tubule cells), respectively, which were labeled as kidney-like cells and were discarded. **I.** GO enrichment analysis for up- and down-regulated genes in C3. Key metabolic processes such as ATP biosynthetic process associated genes are down-regulated and cell cycle related genes are up-regulated in C3, so this clique is removed as cells in cell cycle.

Figure S2 Sexually dimorphic gene expression and gene set enrichment in β cells

A. Barplot showing the cell type composition of male and female mice under different conditions. 8W, 8-week-old; 9M, 9-month-old; 11M, 11-month-old; Endo-islet, endogenous islets of recipients; TX-islet, transplanted islets in recipients. **B.** t-SNE map of retained mouse cells colored by expression of sex chromosome linked genes. The reds for X-chromosome linked gene *Xist*, and the blues for Y-chromosome linked genes *Eif2s3y*, *Ddx3y*, *Uty*. **C.** GSEA for sex comparisons of β cells from 8-week-old C57 mice. The gene sets with NES > 0 are enriched in males and NES < 0 in females. **D.** GSEA for sex comparisons of β cells from healthy 9-month-old C57 mice. The gene

bioRxiv preprint doi: https://doi.org/10.1101/2020.09.22.307421; this version posted September 22, 2020. The copyright holder for this preprint (which was not certified by peer review) is the author/funder. All rights reserved. No reuse allowed without permission.

sets with NES > 0 are enriched in males and NES < 0 in females. **E.** GSEA for sex comparisons of β cells from T2D 9-month-old C57 mice. The gene sets with NES > 0 are enriched in males and NES < 0 in females.

Figure S3 Sexually dimorphic genes in β cells from T2D model and transplanted islet

A. Violin plots of sex-dependent genes in mouse β cells. Top 5 significantly up-regulated and down-regulated T2D altered genes in each group are selected according to the value of FDR. **B.** Violin plots of sex-dependent T2D altered genes involved in ribosome pathway. The left 3 down-regulated genes in female T2D β cells are female-dependent T2D altered genes; the right 11 up-regulated genes in T2D β cells are male-dependent T2D altered genes. **C.** MA plot showing the comparison between sex matched and mismatched transplant-β cells. Up-regulated and down-regulated genes in sex matched transplant-β cells are highlighted in blue and red, respectively. See also in Table S2. TX-β, transplant-β cells. **D.** Violin plot of expression of *Sfrp5* in endogenous and transplanted β cells. M.Endo-β, endogenous β cells from male recipient; F.Endo-β, endogenous β cells from female recipient; Match.TX-β, sex matched transplant-β cells; Mismatch.TX-β, sex mismatched transplant-β cells. **E.** Blood glucose level before and after islet transplantation in diabetic mice. The blood glucose level of diabetic mice with sex-matched (blue) and sex-mismatched (red) transplanted islet are all recovered normal (green baseline) from hyperglycemia (orange baseline) about 3 weeks after transplantation. TX, transplantation.

Table S1 Sex-biased genes and genes overlapped with leading-edge genes of enriched gene sets

Table S2 Sex-independent, sex-dependent T2D altered genes and DEGs of transplant-β cells

Table S3 Primer sequence for library construction